Photochemical & Photobiological Sciences

PAPER

Cite this: *Photochem. Photobiol. Sci.*, 2017, **16**, 555

Photochemical synthesis and photophysical properties of coumarins bearing extended polyaromatic rings studied by emission and transient absorption measurements†

Minoru Yamaji,*[a] Yuma Hakoda,[b] Hideki Okamoto[c] and Fumito Tani[d]

Received 3rd November 2016,
Accepted 16th January 2017

DOI: 10.1039/c6pp00399k

rsc.li/pps

We prepared a variety of coumarin derivatives having expanded π-electron systems along the direction crossing the C_3–C_4 bond of the coumarin skeleton *via* a photochemical cyclization process and investigated their photophysical features as a function of the number (*n*) of the added benzene rings based on emission and transient absorption measurements. Upon increasing *n*, the fluorescence quantum yields of the π-extended coumarins increased. Expanding the π-electron system on the C_3–C_4 bond of the coumarin skeleton was found to be efficient for increasing the fluorescence ability more than that on the C_7–C_8 bond. Introducing the methoxy group at the 7-position was also efficient for enhancing the fluorescence quantum yield and rate of the expanded coumarins. The non-radiative process from the fluorescence state was not substantially influenced by the expanded π-electron system. The competitive process with the fluorescence was found to be intersystem crossing to the triplet state based on the observations of the triplet–triplet absorption. The effects of the expanded π-electron systems on the fluorescence ability were investigated with the aid of TD-DFT calculations.

1. Introduction

Polyaromatic hydrocarbons with extended π-electron systems belong to two major groups from the viewpoint of their molecular shape. One is acenes represented by anthracene, tetracene, and pentacene, which consist of linearly aligned benzene rings. In the last two decades, acenes have been given significant attention because of their potential as organic semiconductor materials, that is, the active layers of organic field effect transistors (OFET)[1–3] although they are generally unstable upon exposure to oxygen and light.[4–6] The other group is phenacenes, such as phenanthrene, chrysene, picene, and fulminene, having benzene rings condensed in a zigzag array. Phenacenes have not been subjected to chemical material research because of the difficulties in their organic synthesis processes until our recent findings. We have reported a facile synthetic process for preparing phenacenes *via* photochemical reactions of diarylethanes using aromatic carbonyls as the photosensitizer (sensitization method),[7] in which chrysene ([4]phenacene), picene ([5]phenacene), and fulminene ([6]phenacene) were readily prepared.[8] We have unveiled that these phenacenes show excellent OFET performance[9,10] and that K-doped picene displays superconductivity at 20 K.[11] Because phenacenes are quite stable on exposure to oxygen and light, they are promising organic electronic materials.[12] It is of interest from the viewpoint of photophysical aspects that picene provides fluorescence emission from the second lowest excited singlet (S_2) state in the vapor phase.[13] However, the phenanthrene skeleton, which is the smallest phenacene, cannot be formed using this method. Instead of the sensitization method, the photocyclization of stilbene derivatives in the presence of oxygen and iodine, which is known as the Mallory photoreaction, is an excellent procedure for the synthesis of phenacene.[14] With this procedure, phenanthrene was readily prepared from stilbene as a precursor of the photoreaction (Scheme 1).

In a previous study, the photophysical features of small phenacenes in solution were investigated.[8] The fluorescence yields were as small as 0.1 irrespective of the number of the benzene rings, *n*, ($3 \leq n \leq 6$). These phenacenes are, thus, not applicable

[a]*Division of Molecular Science, Graduate School of Science and Engineering, Gunma University, Kiryu, Gunma 376-8515, Japan. E-mail: yamaji@gunma-u.ac.jp*
[b]*Education Program of Materials and Bioscience, Graduate School of Science and Engineering, Gunma University, Kiryu, Gunma 376-8515, Japan*
[c]*Division of Earth, Life, and Molecular Sciences, Graduate School of Natural Science and Technology, Okayama University, Okayama 700-8350, Japan*
[d]*Institute for Materials Chemistry and Engineering, Kyushu University, Fukuoka 819-0395, Japan*

†Electronic supplementary information (ESI) available: The precise synthesis procedures and analytical data for the compounds used in this work, the decay profiles of fluorescence, results of DFT calculations including tables of the atom coordinates for the optimized geometries, and the ^{1}H and ^{13}C NMR spectra of the prepared coumarin derivatives. See DOI: 10.1039/c6pp00399k

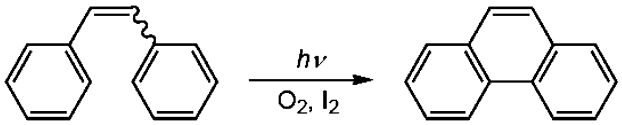

Scheme 1 The photocyclization process to convert stilbene to phenanthrene.

to electronic luminescence (EL) materials although they are durable towards the unfavorable surrounding factors of organic electronic devices such as heat, light, oxygen, and high voltage.

Coumarin and its derivatives have been subjected to photochemical and photophysical studies because of their wide range of applications, such as laser dyes and fluorescent labels, as well as the molecular systems established as important photosensitizers for both *in vitro* and *in vivo* systems.[15–17] A number of photophysical properties of coumarin and its derivatives have been studied by emission and EPR measurements.[18–25] Coumarin shows little fluorescence because the lowest excited singlet (S_1) state of coumarin is an n,π* type.[24] By adding substituents to the coumarin moiety, the electronic character of the S_1 state alters from n,π* to π,π*, resulting in the observation of fluorescence in the blue-green region, which has been exploited as laser dyes[26] and fluorescent probes under various conditions.[27] A recent study, however, has reported that the electronic character of the S_1 state is π,π* based on PBE0 calculations.[28] The directions of the transition moments in the coumarin skeleton are specifically defined.[29] The transition notated as ^1L_b classified by Platt[30] is oblique to the allowed transition ^1L_a, which goes along the axis crossing the C_3–C_4 and C_7–C_8 bonds on the skeleton (see Chart 1).

Therefore, introducing electron donating and withdrawing substituents at the 3- and 7-positions of the coumarin skeleton is a typical strategy for increasing the fluorescence yields, as seen in Coumarins 6, 7, 153, 334 *etc.*, that are used for laser dyes. This methodology is based on the idea of increasing the ^1L_a transition moment by expanding the π-electron system along the direction of the ^1L_a transition. However, these substituted coumarins are labile to surrounding factors. A superior methodology, such as phenacenes, for enhancing the emission properties and increasing the durability to the surrounding stimuli is required for designing coumarins as efficient and robust fluorophores applicable to EL devices.

In this context, we synthesized a variety of coumarins having extended π-electron systems in a zig-zag style, like the phenacenes, on the C_3–C_4 and C_7–C_8 bonds of the skeleton *via* the photocyclization of aryl-coumarinylethenes. Some of these coumarins were substituted with a methoxy group at the 7-position. The molecular structures of the prepared coumarins are illustrated in Chart 2. The photophysical features of the prepared coumarins were studied by measuring the fluorescence yield, lifetimes, and transient absorption in the solution. The origins of the increasing fluorescence ability of these coumarins are discussed with the aid of theoretical calculations.

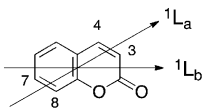

Chart 1 The directions of the transition moments on the coumarin skeleton.

2. Experimental

Materials

The coumarin derivatives used in this study were prepared, with the exception of commercially available CM[0] and MeOCM[0], according to the procedures described in the ESI.†

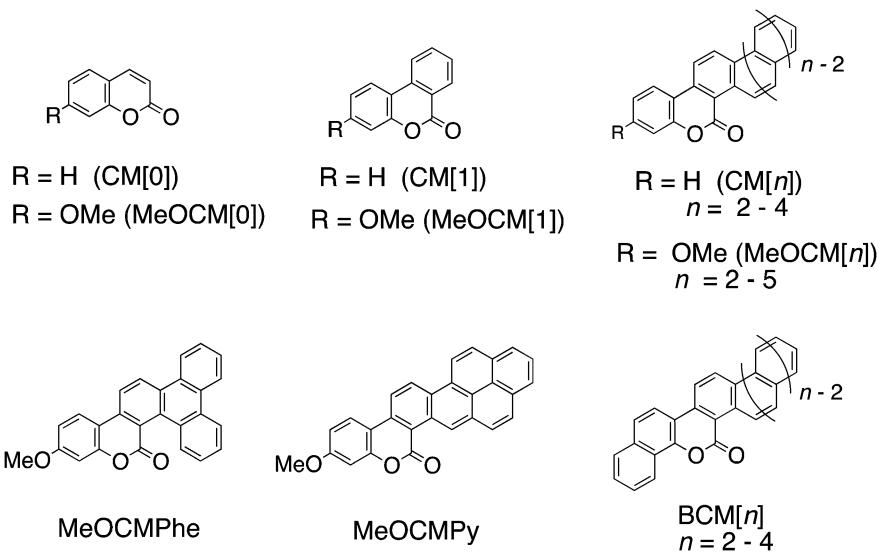

Chart 2 The molecular structures and abbreviations of the coumarin derivatives used in this study.

Spectroscopic grade chloroform and ethanol from Kishida were used as supplied. We used only chloroform as the solvent for obtaining the electronic spectra and transient absorption spectra at room temperature because some of the newly prepared compounds showed little solubility in the common organic solvents other than chloroform. EtOH was used as a matrix for the phosphorescence measurements at 77 K. The sample solutions in a quartz cuvette with 1 cm path length were freshly prepared and purged by bubbling pure Ar.

Instrumentation

The absorption and emission spectra were obtained using a JASCO V-550 spectrophotometer and a Hitachi F-4010 fluorescence spectrophotometer, respectively. Nanosecond fluorescence lifetimes (τ_f) were determined using a time-correlated single-photon counting fluorimeter (C12132 from Hamamatsu Photonics). Fluorescence quantum yields (Φ_f) were determined using an absolute luminescence quantum yield measurement system (C9920-02) from Hamamatsu Photonics.[31] A XeCl excimer laser (308 nm, 17 mJ per pulse, FWHM 20 ns, Lextra 50 from Lambda Physik) was used as the light source for flash photolysis. The number of laser pulses in each sample was less than four to avoid excess exposure. Details of the detection system used for the time profiles of the transient absorption have been reported elsewhere.[32] The transient absorption spectra were obtained using TSP-1000M from Unisoku, which provides a transient absorption spectrum with one laser pulse. The transient data obtained upon laser flash photolysis were analyzed using the least-squares best-fitting method. Measurements of the fluorescence and transient absorption were carried out at 295 K. The ^{1}H- (600 MHz) and ^{13}C- (150 MHz) NMR spectra were obtained using a VARIAN NMR SYSTEM 600 spectrometer. The residual solvent protons were used as an internal standard and the chemical shifts (δ) are given relative to tetramethylsilane (TMS). Coupling constants (J) are given in hertz. High-resolution fast atom bombardment

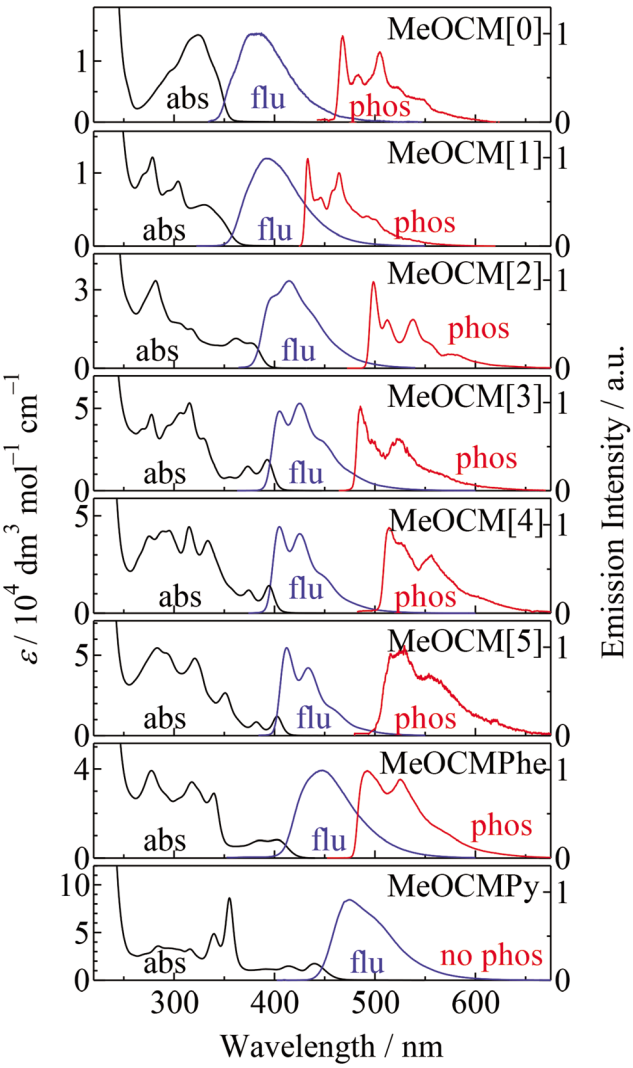

Fig. 1 The absorption and fluorescence spectra obtained in $CHCl_3$ at 295 K and the phosphorescence spectra were obtained in ethanol at 77 K for MeOCM[n] ($0 \leq n \leq 5$), MeOCMPhe and MeOCMPy.

Table 1 The photophysical parameters obtained in $CHCl_3$ [a]

Compound	ε/dm^3 mol^{-1} cm^{-1} (λ_{abs}/nm)	λ_{flu}/nm	Φ_f	τ_f/ns	k_f/10^8 s^{-1}	Φ_{nr}	k_{nr}/10^8 s^{-1}	E_S/kcal mol^{-1}	E_T/kcal mol^{-1}	τ_T/μs
MeOCM[0]	14 500(323)	380	0.014	N/A	N/A	0.99	N/A	81.7	60.9	N/A
MeOCM[1]	12 100(279)	391	0.091	1.3	0.70	0.91	7.0	82.8	65.8	4.0
MeOCM[2]	33 700(280)	414	0.11	1.1	1.0	0.89	8.1	76.0	57.2	12.0
MeOCM[3]	53 500(315)	424	0.27	2.1	1.3	0.73	3.5	73.9	58.7	11.0
MeOCM[4]	44 300(315)	404	0.27	2.3	1.2	0.73	3.2	73.5	55.4	8.6
MeOCM[5]	55 300(282)	412	0.40	3.0	1.3	0.60	2.0	72.0	54.0	12.0
MeOCMPhe	39 700(276)	446	0.05	0.67	0.75	0.95	14.2	68.7	57.9	5.4
MeOCMPy	86 100(355)	473	0.18	1.9	0.94	0.82	4.3	63.3	N/A	8.7
CM[0]	11 600(274)	N/A	N/A	N/A	N/A	N/A	N/A	85.5	N/A	N/A
CM[1]	14 500(272)	380	0.002	<0.3	>0.07	~1.0	>33.3	83.9	66.5	N/A
CM[2]	49 500(274)	387	0.012	<0.3	>0.4	0.99	>33.0	78.0	57.3	18.8
CM[3]	37 500(295)	392	0.16	2.6	0.62	0.84	3.2	74.6	56.7	6.1
CM[4]	39 900(295)	415	0.14	3.9	0.36	0.86	2.2	73.8	55.1	7.7
BCM[2]	72 000(277)	430	0.04	0.45	0.84	0.96	21.4	71.6	55.5	6.2
BCM[3]	50 100(271)	430	0.06	0.58	1.1	0.94	16.1	70.7	56.7	6.3
BCM[4]	56 600(276)	433	0.10	0.77	1.3	0.90	11.7	70.3	55.1	5.0

[a] Experimental errors, within ±5%.

mass spectra (HR-FAB-MS) were obtained using 3-nitrobenzyl alcohol (NBA) as a matrix *via* a JEOL JMS-700 spectrometer. Melting points were measured *via* a Yanaco MP-S3 melting point apparatus.

Theoretical calculations

Calculations were carried out at the DFT level using the Gaussian 09 software package.[33] The geometries of the coumarin derivatives were fully optimized using the 6-31+G(d) basis set at the B3LYP level in vacuum. The atom coordinates for the optimized geometries are deposited in the ESI.† TD-DFT calculations were performed at the TD B3LYP/6-31+G(d) level of theory using the optimized geometries.

3. Results and discussion

Absorption and emission spectra

Fig. 1 shows the absorption and emission spectra of the MeOCMs used in the present study.

The absorption and emission spectra obtained for CM[*n*] and BCM[*n*] are deposited in the ESI as Fig. S1 and 2,† respectively. The observed absorption bands show large absorption coefficients, ε, in the magnitude of 10^4 dm^3 mol^{-1} cm^{-1} (Table 1), which are due to the allowed π–π* transition (the ^1L_a band). Upon increasing the number of benzene rings, *n*, in MeOCM[*n*], CM[*n*], and BCM[*n*], the onsets of the absorption spectra red-shifted until *ca.* 420 nm as well as those of MeOCMPhe and MeOCMPy to longer wavelengths. These shifts may originate from the π-electron systems being expanded on the 3- and 4-positions of the coumarin skeleton. Based on the fact that all the compounds, except for coumarin (CM[0]), show fluorescence, the electronic character of the S_1 state was assigned to be π,π*. Phosphorescence was observed from all the compounds, except for MeOCMPy and CM[0], indicating that the intersystem crossing from the S_1 state to the lowest triplet (T_1) state was efficient in a rigid matrix at 77 K. From the origins of fluorescence and phosphorescence spectra, the S_1 and T_1 state energies (E_S and E_T, respectively) were determined and are listed in Table 1.

The quantum yields (Φ_f) and lifetimes (τ_f) of the fluorescence were determined in $CHCl_3$. The decay profiles of the fluorescence are deposited in the ESI.† Based on these parameters, the fluorescence rate (k_f), quantum yield (Φ_{nr}), and rate (k_{nr}) for the non-radiative processes were evaluated using eqn (1)–(3), respectively.

$$k_f = \Phi_f \tau_f^{-1} \quad (1)$$

$$\Phi_{nr} = 1 - \Phi_f \quad (2)$$

$$k_{nr} = \Phi_{nr} \tau_f^{-1} \quad (3)$$

These values are also listed in Table 1.

Fig. 2 shows the plots of the photophysical parameters obtained for comparison.

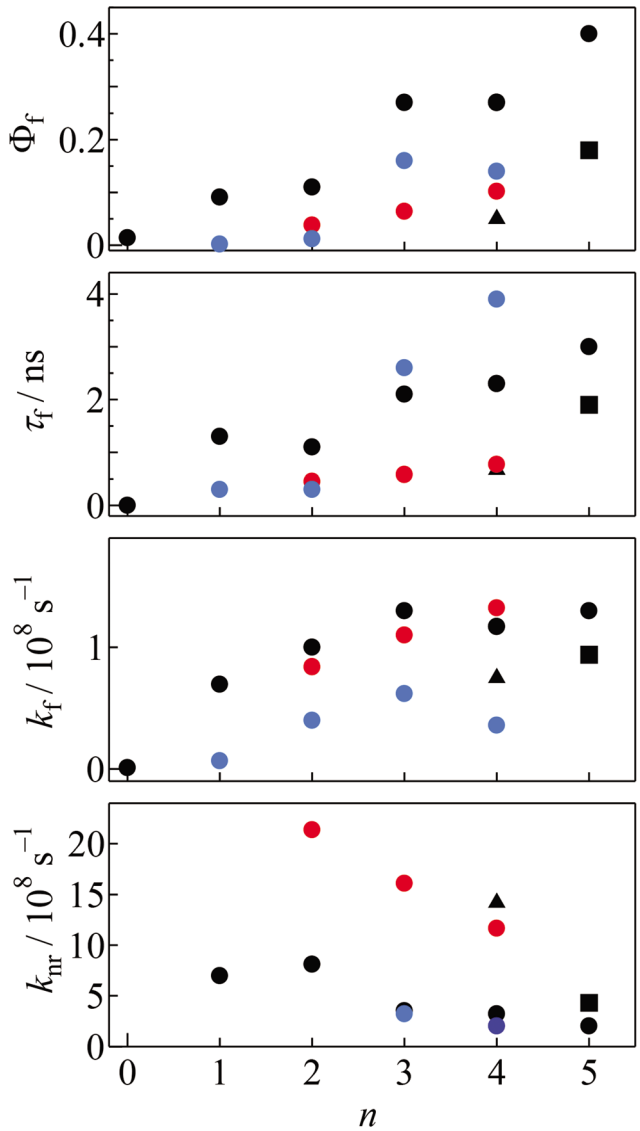

Fig. 2 The quantum yields (Φ_f), lifetimes (τ_f) and rates (k_f) for fluorescence, and rates (k_{nr}) for the non-radiative processes obtained in $CHCl_3$ determined for MeOCM[*n*] (●; $0 \le n \le 5$), MeOCMPhe (▲; $n = 4$), MeOCMPy (■; $n = 5$), CM[*n*] (●; $0 \le n \le 4$) and BCM[*n*] (●; $2 \le n \le 4$) plotted as a function of the number of benzene rings, *n*. The plots of k_{nr} for CM[1] and CM[2] are out of the ordinate.

Upon increasing *n* for MeOCM[*n*], the Φ_f value increased from 0.01 to 0.4. The Φ_f value (~0.15) of CM[3] was similar to that of CM[4], whereas those of CM[0–3] were close to zero. The Φ_f value obtained for BCM[*n*] moderately increased with the increasing *n*. These results indicate that the linearly expanded π-electron system with more than three benzene rings on the C_7–C_8 bonds of the coumarin skeleton is efficient in enhancing the Φ_f values. Conversely, the Φ_f values of MeOCMPhe and MeOCMPy are, respectively, smaller than those of the isomeric MeOCM[4] and MeOCM[5]. These facts indicate that the two-dimensional expansion of the π-electron system is less efficient for enhancing the fluorescence

quantum yield when compared with the phenacene-like extension. It seems that expanding the π-electron system also works for elongating the fluorescence lifetime, τ_f. The important photophysical parameter for characterizing the fluorescence properties is the fluorescence rate, k_f, evaluated from the Φ_f and τ_f values using eqn (1). As increasing the n, the k_f value increased. For MeOCM[n], the k_f value leveled off at 1.3×10^8 s^{-1} for n = 3–5. The k_f values of MeOCMPhe and MeOCMPy are, respectively, smaller than those of the isomeric MeOCM[4] and MeOCM[5]. These facts also indicate that expanding the π-electron system in a non-zigzag style is less efficient for enhancing the fluorescence ability when compared with the

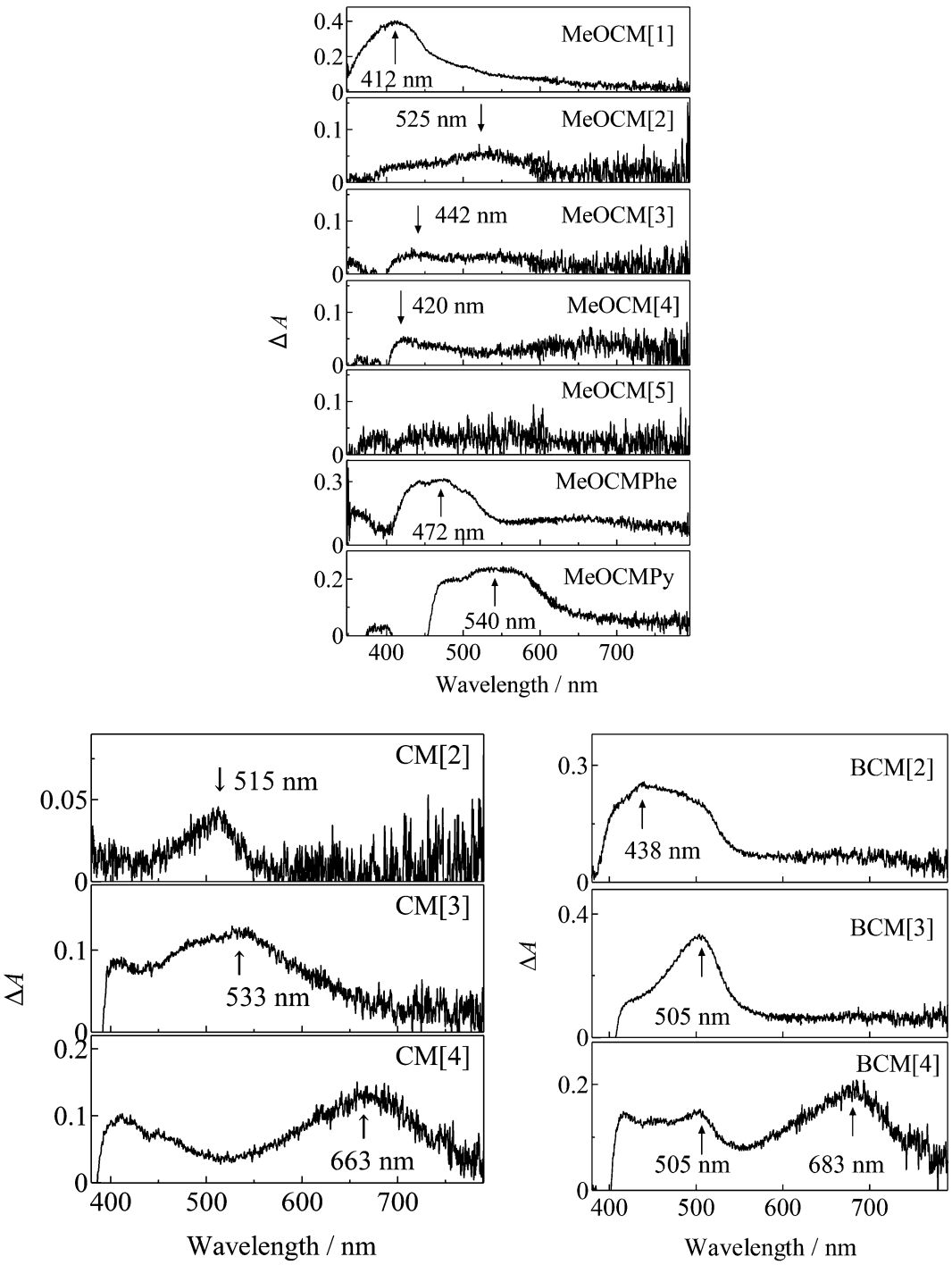

Fig. 3 The transient absorption spectra obtained at 200 ns upon 308 nm laser excitation in an Ar-purged $CHCl_3$ solution of the coumarin derivatives.

phenacene-like extension. The k_f values for CM[n] are smaller than those of the corresponding MeOCM[n] and BCM[n]. These facts demonstrate that adding electron-donating substituents at the 7-position and expanding the π-electron system on the C_7–C_8 bonds of the coumarin skeleton are efficient for increasing the ^1L_a transition moment (see Chart 1 for the direction), which is closely related to the k_f value obtained with the Strickler–Berg relationship.[34] As with the k_{nr} values of MeOCM[n], those for n = 3–5 were suppressed to 2–3 × 10^8 s^{-1} when compared to those obtained for n = 0–2. This feature in the k_{nr} value is contrary to that in the k_f value, which shows a leveling off at larger n values. The k_{nr} values of BCM[2–4] are substantially larger than those of the MeOCM[n] and CM[n] at their corresponding n values. The difference in the k_{nr} values may be due to the benzene moiety on the C_7–C_8 bond of BCM [n]. Consequently, it was found that expanding the π-electron system on the C_7–C_8 bond of the coumarin skeleton does not enhance the fluorescence ability, whereas increases the k_{nr} value.

Observation of triplet formation in the transient absorption measurements

In the present study, the effects of the extended π-electron systems on the non-radiative processes, which may comprised internal conversion (IC) to the ground state and intersystem crossing (ISC) to the triplet states, were examined by observing the triplet–triplet (T–T) absorption using flash photolysis techniques. Fig. 3 shows the transient absorption spectra obtained at 200 ns upon laser photolysis of the $CHCl_3$ solutions of the coumarin derivatives prepared in this study.

The transient absorption spectra of the studied compounds, with the exception of MeOCM[0], CM[0], and CM[1], were obtained in the wavelength region of 380–800 nm. The intensities of all the transient absorptions decreased with lifetimes (τ_T) in the microsecond time domain (Table 1) and the decay was accelerated in the presence of dissolved oxygen. From these observations, the obtained transient signals could be ascribed to the T–T absorption of the studied compounds. Observation of the triplet state in solution indicates that ISC from the S_1 to the T_1 state competes with the fluorescence process. Therefore, it was apparent that the non-radiative rates (k_{nr}) from the S_1 states are due to ISC to the T_1 states. The absence of the T–T absorption spectra for MeOCM[0], CM[0], and CM[1] demonstrates that IC from the S_1 state to the ground state was dominant.

DFT calculations for the excited singlet states

To obtain an insight into the photophysical properties of the studied coumarin derivatives, density functional theory (DFT) was used to calculate the electronic structures and time-depen-

Table 2 The results of the TD-DFT calculations performed in vacuum

Compound	HOMO/eV	LUMO/eV	Energy gap/eV	$S_1 \leftarrow S_0$ transition	λ_{tr}/nm (f)	Configuration[a]
MeOCM[0]	−2.70	−1.00	1.70	π,π*	305(0.3281)	H → L (0.67895) H−1 → L (0.13581)
MeOCM[1]	−2.57	−0.92	1.64	π,π*	371(0.1300)	H → L (0.69283)
MeOCM[2]	−2.53	−1.03	1.50	π,π*	348(0.1706)	H → L (0.67676) H → L+1 (−0.12048) H−1 → L+1 (−0.10629)
MeOCM[3]	−2.53	−1.00	1.53	π,π*	400(0.2526)	H → L (0.65950) H−1 → L (−0.13479) H−1 → L+1 (0.18085)
MeOCM[4]	−2.48	−1.05	1.43	π,π*	431(0.0911)	H → L (0.68217) H−1 → L (−0.13637)
MeOCM[5]	−2.45	−1.04	1.41	π,π*	439(0.2122)	H → L (0.69072) H−1 → L (−0.10979)
MeOCMPhe	−2.46	−1.05	1.41	π,π*	382(0.2406)	H → L (0.68242)
MeOCMPy	−2.31	−1.11	1.20	π,π*	498(0.1969)	H → L (0.67723) H → L+1 (−0.17557)
CM[0]	−2.91	−0.96	1.95	π,π*	300(0.1205)	H → L (0.64119) H−1 → L (0.25551) H−1 → L+1 (−0.11875)
CM[1]	−2.82	−0.83	1.98	π,π*	300(0.1646)	H → L (0.65171) H → L+1 (0.16624) H−1 → L+1 (−0.10153) H−2 → L (0.11244) H−2 → L+1 (−0.11286)
CM[2]	−2.64	−1.10	1.53	π,π*	381(0.0965)	H → L (0.69003)
CM[3]	−2.61	−1.05	1.56	π,π*	396(0.1704)	H → L (0.67146) H−1 → L+1 (0.19916)
CM[4]	−2.50	−1.09	1.42	π,π*	437(0.0793)	H → L (0.69165)
BCM[2]	−2.44	−1.15	1.29	π,π*	450(0.1395)	H → L (−0.70103)
BCM[3]	−2.42	−1.14	1.28	π,π*	452(0.1994)	H → L (−0.70062)
BCM[4]	−2.49	−1.08	1.42	π,π*	435(0.0801)	H → L (0.67284) H−1 → L (−0.17200)

[a] The abbreviations H and L indicate the HOMO and LUMO, respectively.

dent DFT (TD-DFT) was adopted to investigate the electronic transitions from the ground to the excited states. The calculated results are summarized in Table 2.

Fig. 4 shows the calculated molecular orbital surfaces for the studied coumarin derivatives showing the highest occupied molecular orbitals (HOMO)

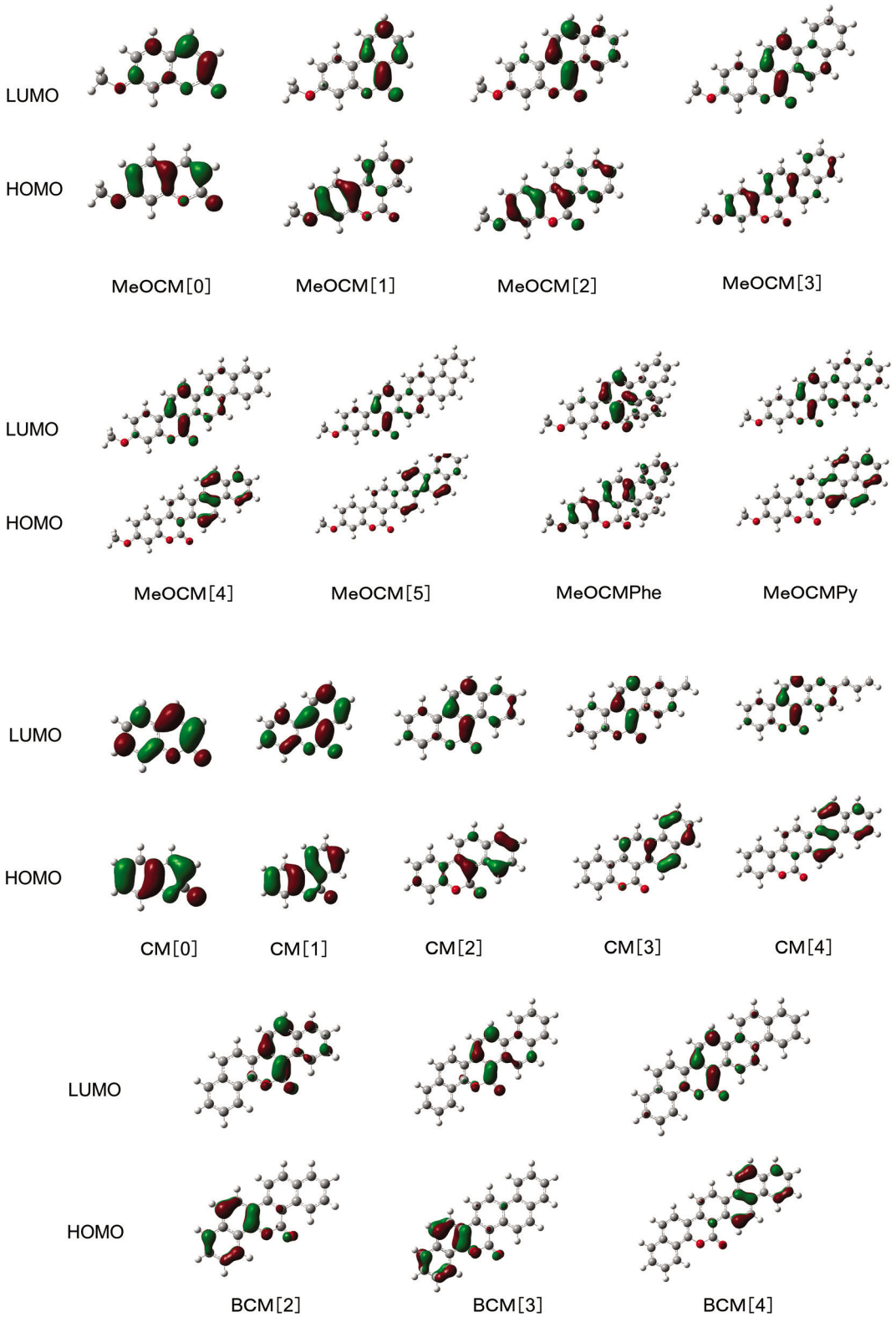

Fig. 4 The HOMO and LUMO surfaces calculated for the coumarin derivatives in vacuum.

and lowest unoccupied molecular orbitals (LUMO) in vacuum.

The $S_1 \leftarrow S_0$ transitions of the studied compounds obtained from the HOMO → LUMO configurations were characterized to be π,π*. Interestingly, in the optimized structures of MeOCM[4], MeOCM[5], MeOCMPy, CM[3], CM[4], and BCM[4], which have relatively large expanded π-electron systems, the π-cloud in the HOMOs were mainly localized on the expanded π-electron moieties and not on the coumarin moieties. This finding demonstrates that the electronic nature in the $S_0 \leftarrow S_1$ transitions of the π-expanded coumarins studied in this study were contributed not from that of coumarin but from the additional π-extension part. Consequently, joining the coumarin moiety together with the phenacene ones *via* the employed photocyclization procedure results in the increasing Φ_f values of the π-extended coumarin systems.

4. Conclusions

We prepared three types of coumarins (MeOCM[*n*], CM[*n*], and BCM[*n*]) having expanded π-electron systems and investigated their photophysical features in solution. Based on the Φ_f and τ_f values, the k_f and k_{nr} values were determined. We observed that upon increasing *n*, the k_f values increased, whereas the k_{nr} decreased in the same series of the coumarin derivatives. Introducing a methoxy group at the 7-position was more efficient for enhancing the Φ_f and k_f values when compared to expanding the π-electron system on the C_7–C_8 bond. Conversely, the k_{nr} values of BCM[*n*] prepared according to the latter tactics were greater than those of MeOCM[*n*] fabricated based on the former tactics. The observed effects of expanding the π-electron systems on the fluorescence ability were understood by considering the location of the HOMO and LUMO surfaces. Upon increasing *n*, the π-electrons in the HOMOs mainly localize on the expanded π-electron moieties, leading to an absence of electronic character in the original coumarin chromophore that causes internal conversion from the S_1 state to the ground state to show no fluorescence and triplet formation. Previously, we reported that the fluorescence quantum yields of phenacenes are as small as 0.1 in $CHCl_3$ irrespective of the number of the benzene rings.[8] The studied MeOCM[*n*] and CM[*n*] for $n \geq 3$ showed Φ_f values (>0.1) larger than those of the parent phenacenes. As a result, we succeeded in increasing the fluorescence ability of both coumarin and phenacenes by this unique strategy, *i.e.*, expanding phenacene-type π-electron systems on the coumarin skeleton.

Acknowledgements

This work has been supported by a Grant-in-Aid for Scientific Research (JP26288032) from the Ministry of Education, Culture, Sports, Science and Technology (MEXT) of Japanese Government to MY. MY acknowledges the technical staff at the Kyushu University for performing the HRMS spectrometry of the new compounds under the Cooperative Research Program of the Network Joint Research Center for Materials and Devices. HO thanks the Okayama Foundation for Science and Technology for financial support.

References

1 Y. Y. Lin, D. J. Gundlach, S. F. Nelson and T. N. Jackson, Stacked pentacene layer organic thin-film transistors with improved characteristics, *IEEE Electron Device Lett.*, 1997, **18**, 606–608.
2 Y. Yamashita, Organic semiconductors for organic field-effect transistors, *Sci. Tecnol. Adv. Mater.*, 2007, **10**, 024313.
3 M. Kitamura and Y. Arakawa, Pentacene-based organic field-effect transistors, *J. Phys.: Condens. Matter*, 2008, **20**, 184011.
4 R. Mondal, B. K. Shah and D. C. Neckers, Photogeneration of heptacene in a polymer matrix, *J. Am. Chem. Soc.*, 2006, **128**, 9612–9613.
5 R. Mondal, C. ToÃànshoff, D. Khon, D. C. Neckers and H. F. Bettinger, Synthesis, stability, and photochemistry of pentacene, hexacene, and heptacene: A matrix isolation study, *J. Am. Chem. Soc.*, 2009, **131**, 14281–14289.
6 C. Tönshoff and H. F. Bettinger, Photogeneration of octacene and nonacene, *Angew. Chem., Int. Ed.*, 2010, **49**, 4125–4128.
7 H. Okamoto, M. Yamaji, S. Gohda, Y. Kubozono, N. Komura, K. Sato, H. Sugino and K. Satake, Facile synthesis of picene from 1,2-di(1-naphthyl)ethane by 9-fluorenone-sensitized photolysis, *Org. Lett.*, 2011, **13**, 2758–2761.
8 H. Okamoto, M. Yamaji, S. Gohda, K. Sato, H. Sugino and K. Satake, Photochemical synthesis and electronic spectra of fulminene ([6]phenacene), *Res. Chem. Intermed.*, 2013, **39**, 147–159.
9 H. Okamoto, N. Kawasaki, Y. Kaji, Y. Kubozono, A. Fujiwara and M. Yamaji, Air-assisted high-performance field-effect transistor with thinfilms of picene, *J. Am. Chem. Soc.*, 2008, **130**, 10470–10471.
10 N. Komura, H. Goto, X. He, H. Mitamura, R. Eguchi, Y. Kaji, H. Okamoto, Y. Sugawara, S. Gohda, K. Sato and Y. Kubozono, Characteristics of [6]phenacene thin film field-effect transistor, *Appl. Phys. Lett.*, 2012, **101**, 083301–083304.
11 R. Mitsuhashi, Y. Suzuki, Y. Yamanari, H. Mitamura, T. Kambe, N. Ikeda, H. Okamoto, A. Fujiwara, M. Yamaji, N. Kawasaki, Y. Maniwa and Y. Kubozono, Superconductivity in alkali-metal-doped picene, *Nature*, 2010, **464**, 76–79.
12 Y. Kubozono, H. Mitamura, X. Lee, X. He, Y. Yamanari, Y. Takahashi, Y. Suzuki, Y. Kaji, R. Eguchi, K. Akaike, T. Kambe, H. Okamoto, A. Fujiwara, T. Kato, T. Kosugi and H. Aoki, Metal-intercalated aromatic hydrocarbons: A new class of carbon-based superconductors, *Phys. Chem. Chem. Phys.*, 2011, **13**, 16476–16493.

13 T. Itoh, M. Yamaji and H. Okamoto, S_2 fluorescence from picene vapor, *Chem. Phys. Lett.*, 2013, **570**, 26–28.
14 F. B. Mallory and C. W. Mallory, *Org. React.*, 1983, **30**, 1.
15 A. C. Giese, Photosensitization of natural pigments, *Photophysiology*, 1971, **6**, 77–129.
16 P.-S. Song, M. L. Harter, T. A. Moore and W. C. Herndon, Luminescence spectra and photocycloaddition of the ecited coumarins to dns bases, *Photochem. Photobiol.*, 1971, **14**, 521–530.
17 M. Lee, M. C. Roldan, M. K. Haskell, S. R. McAdam and J. A. Hartley, In vitro photoinduced cytotoxicity and DNA binding properties of psoralen and coumarin conjugates of netropsin analogues: DNA sequence-directed alkylation and cross-link formation, *J. Med. Chem.*, 1994, **37**, 1208–1213.
18 D. R. Graber, M. W. Grimes and A. Haug, Electron paramagnetic resonance studies of the triplet state of coumarin and related compounds, *J. Chem. Phys.*, 1969, **50**, 1623–1626.
19 J. B. Gallivan, Spectroscopic studies on coumarin, *Mol. Photochem.*, 1970, **2**, 191–211.
20 P.-S. Song and W. H. Gordon, Spectroscopic study of the excited states of coumarin, *J. Phys. Chem.*, 1970, **74**, 4234–4240.
21 W. W. Mantulin and P.-S. Song, Excited states of skin-sensitizing coumarins and psoralens. Spectroscopic studies, *J. Am. Chem. Soc.*, 1973, **95**, 5122–5129.
22 E. T. Harrigan, A. Chakrabarti and N. Hirota, Single crystal EPR, zero-field ODMR, and phosphorescence studies of the T1 state of coumarin, *J. Am. Chem. Soc.*, 1976, **98**, 3460–3465.
23 A. D. Marques and G. S. Marques, Spectroscopic studies of coumarin in micelles, *Photochem. Photobiol.*, 1994, **59**, 153–160.
24 J. S. Séixas de Melo, R. S. Becker and A. L. Maçanita, Photophysical behavior of coumarins as a function of substitution and solvent: Experimental evidence for the existence of a lowest lying $^1(n,\pi^*)$ state, *J. Phys. Chem.*, 1994, **98**, 6054–6058.
25 A. Satpati, S. Senthilkumar, M. Kumbhakar, S. Nath, D. K. Maity and H. Pal, Investigations of the solvent polarity effect on the photophysical properties of coumarin-7 dye, *Photochem. Photobiol.*, 2005, **81**, 270–278.
26 F. Bayrakçeken, A. Yaman and M. Hayvali, Photophysical and photochemical study of laser-dye coumarin-481 and its photoproduct in solution, *Spectrochim. Acta, Part A*, 2005, **61**, 983–987.
27 A. S. Vasylevska, A. A. Karasyov, S. M. Borisov and C. Krause, Novel coumarin-based fluorescent ph indicators, probes and membranes covering a broad pH range, *Anal. Bioanal. Chem.*, 2007, **387**, 2131–2141.
28 A. D. Laurent, C. Adamo and D. Jacquemin, Dye chemistry with time-dependent density functional theory, *Phys. Chem. Chem. Phys.*, 2014, **16**, 14334–14356.
29 B. Valeur, *Molecular fluorescence: Principles and applications*, Wiely-VCH, Weinheim, 2002.
30 J. R. Platt, Classification of spectra of cata-condensed hydrocarbons, *J. Phys. Chem.*, 1949, **17**, 484–495.
31 K. Suzuki, A. Kobayashi, S. Kaneko, K. Takehira, T. Yoshihara, H. Ishida, Y. Shiina, S. Oishi and S. Tobita, Reevaluation of absolute luminescence quantum yields of standard solutions using a spectrometer with an integrating sphere and a back-thinned ccd detector, *Phys. Chem. Chem. Phys.*, 2009, **11**, 9850–9860.
32 M. Yamaji, Y. Aihara, T. Itoh, S. Tobita and H. Shizuka, Thermochemical profiles on hydrogen atom transfer from triplet naphthol and proton-induced electron transfer from triplet methoxynaphthalene to benzophenone via triplet exciplexes studied by laser flash photolysis, *J. Phys. Chem.*, 1994, **98**, 7014–7021.
33 M. J. Frisch, G. W. Trucks, H. B. Schlegel, G. E. Scuseria, M. A. Robb, J. R. Cheeseman, G. Scalmani, V. Barone, B. Mennucci, G. A. Petersson, H. Nakatsuji, M. Caricato, X. Li, H. P. Hratchian, A. F. Izmaylov, J. Bloino, G. Zheng, J. L. Sonnenberg, M. Hada, M. Ehara, K. Toyota, R. Fukuda, J. Hasegawa, M. Ishida, T. Nakajima, Y. Honda, O. Kitao, H. Nakai, T. Vreven, J. J. A. Montgomery, J. E. Peralta, F. Ogliaro, M. Bearpark, J. J. Heyd, E. Brothers, K. N. Kudin, V. N. Staroverov, T. Keith, R. Kobayashi, J. Normand, K. Raghavachari, A. Rendell, J. C. Burant, S. S. Iyengar, J. Tomasi, M. Cossi, N. Rega, J. M. Millam, M. Klene, J. E. Knox, J. B. Cross, V. Bakken, C. Adamo, J. Jaramillo, R. Gomperts, R. E. Stratmann, O. Yazyev, A. J. Austin, R. Cammi, C. Pomelli, J. W. Ochterski, R. L. Martin, K. Morokuma, V. G. Zakrzewski, G. A. Voth, P. Salvador, J. J. Dannenberg, S. Dapprich, A. D. Daniels, O. Farkas, J. B. Foresman, J. V. Ortiz, J. Cioslowski and D. J. Fox, *Gaussian 09, revision D.01*, Gaussian, Inc., Wallingford CT, 2010.
34 S. J. Strickler and R. A. Berg, Relationship between absorption intensity and fluorescence lifetime of molecules, *J. Phys. Chem.*, 1962, **37**, 814–822.